



Title	Lens Effect Artifact in Ultrasonography as Produced by Rectus Abdominis Muscle
Author(s)	東, 義孝
Citation	日本医学放射線学会雑誌. 1986, 46(6), p. 825-838
Version Type	VoR
URL	https://hdl.handle.net/11094/17243
rights	
Note	

The University of Osaka Institutional Knowledge Archive : OUKA

<https://ir.library.osaka-u.ac.jp/>

The University of Osaka

Lens Effect Artifact in Ultrasonography as Produced by Rectus Abdominis Muscle

Yoshitaka Higashi

Department of Radiology, Faculty of Medicine, Fukuoka University

Research Code No. : 208.3

Key Words : *Ultrasonic artifact, Refraction artifact, Double image artifact, Lens effect artifact*

超音波画像にみられる新しいアーチファクト

—腹直筋のレンズ効果—

福岡大学医学部放射線科

東 義 孝

（昭和60年11月13日受付）

（昭和61年1月22日最終原稿受付）

上腹部の超音波検査時に、正中線の後方の構造が二重に描出される現象が認められる。

このアーチファクトはリニア電子スキャナで検査すると高頻度に出現し、画像の読影を誤らせる危険性がある重要な現象である。

この現象の成因を明らかにするために、臨床例を収集して発生状況を観察したところ、腹直筋が関与していることが判明した。ファントムを作

成して実験した結果、このアーチファクトが再現され、腹直筋が音響レンズの役割をして超音波を屈折させていることが明確になった。スネルの法則に基づいて腹直筋を通過する超音波の屈折角を求める理論式を立て、臨床例で理論値と実測値が一致することを確認した。

著者はこの現象をレンズ効果と名付けた。

Introduction

An ultrasonic beam incident on the body surface is reflected at various interfaces between tissues due to their different acoustic impedances. The reflected beams are then processed electronically and displayed on the video monitor of the ultrasonic equipment.

Ultrasonic equipment is designed on the basis of the following assumptions¹⁾:

All tissues permit an acoustic velocity of 1,540 m/s.

An ultrasonic beam propagates in a straight line without changing its direction in the body.

All reflectors which are detected are in the central axis of the transducer's beam.

An ultrasonic beam is detected after it is reflected only once at the reflector within the body.

These assumptions are nearly correct; however, on strict interpretation, each of them is not entirely true. For example, with the first assumption, the mean sound velocity in soft tissue is 1,540 m/s, but each organ and each tissue has a characteristic sound velocity, varying in a range from 10 to 90 m/s. In the case of the second assumption, the ultrasonic beam which strikes interfaces between different tissues obliquely, each with its own sound velocity, is refracted so that it does not proceed in a straight line. In the case of the third

assumption, since the ultrasonic beam has several adjacent lobes, any strong reflector located slightly distant from the central axis of the beam will be displayed as though it were located precisely in the beam's central axis. Regarding the fourth assumption, some of the ultrasonic beam reflected within the body will again be reflected at another reflector, or at the anterior surface of the probe on its way to the transducer.

Several phenomena mitigate against the above assumptions which are used for equipment design. That which does not exist within the body will be displayed as if it were an existing image, or the image will be distorted. These phenomena result in artifacts sometimes called "ghosts". From an engineering standpoint, it is difficult to exclude them entirely.

During the interpretation of ultrasonic images, the existence of mechanisms resulting in artifacts must be recognized. We must take care not to be confused by them, and we must not misinterpret their images.

An artifact is created based on the phenomenon that during a transverse scan the structures in midline immediately posterior to the surface are visualized as double images. This artifact is often produced during examinations using linear arrays. It is quite possible that this phenomenon can result in misinterpretations of ultrasonic images.

We have termed this artifact the "lens effect", and studied its cause by clinical observations; by imaging a tissue-equivalent phantom; and by reviewing the pertinent physics.

Clinical Manifestations of the Lens Effect

1. Method

Two linear arrays (Yokogawa RT 2000 and Aloka SSD 256), one linear and phased array (Yokogawa RT 3000) and one contact compound scanner (Siemens Pho/Sonic) were used. Each transducer operated at a frequency of 3.5 MHz.

Patients were carefully scanned to verify that their vascular structures were clearly visualized in midline during transverse scans. Care was taken to consider the timing of each patient's respirations, and the angulation of the probe.

When blood vessels were displayed as double images, the images were "frozen" and recorded on multifilm. Images of the same structures in the same patients but free of such artifacts were also recorded.

2. Results

Among 1,299 upper abdominal ultrasonographic examinations performed during four months in the Department of Diagnostic Radiology, Fukuoka University Hospital, double images were observed in 62 transverse scans.

In nearly all of the 1,237 patients in whom this artifact was not recognized, intestinal gas interfered with the imaging of the blood vessels, or the blood vessels were not located directly beneath the linea alba.

Double images of the mesenteric arteries were observed in 31 cases; of the umbilical portion of the intrahepatic portal vein in 27 cases; of the celiac axis in four cases; of the left hepatic vein in two cases; and of the aorta in 20 cases. In ten patients the aorta was visualized as ovoid, or as two round overlapping structures.

In the present study, patients with minimal deformities of the aorta were excluded. Double images of the caudate lobe of the liver and of the vertebral column were also observed, but they were likewise excluded because double images in these cases were not so demonstrable to explain the "lens effect".

Case 1

Generally, the abdominal aorta is visualized as a round structure (Fig. 1a); but, when it is located directly beneath the linea alba (Fig. 1b), it is visualized as two round structures, side-by-side.

Case 2

The superior mesenteric artery is normally visualized as in Fig. 2a; however, it is imaged as two round

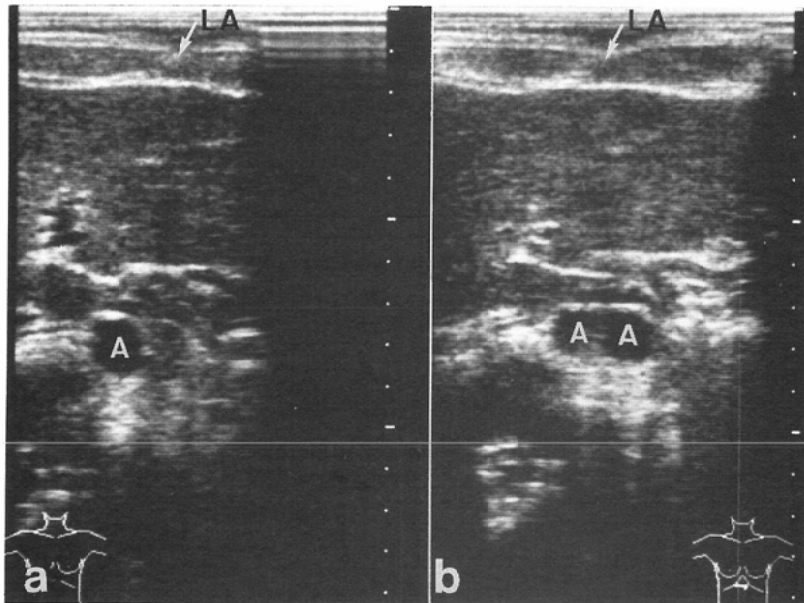


Fig. 1 Case 1. a, The abdominal aorta is visualized as a round structure. b, The abdominal aorta is visualized as two round structures. A=aorta; LA=linea alba.

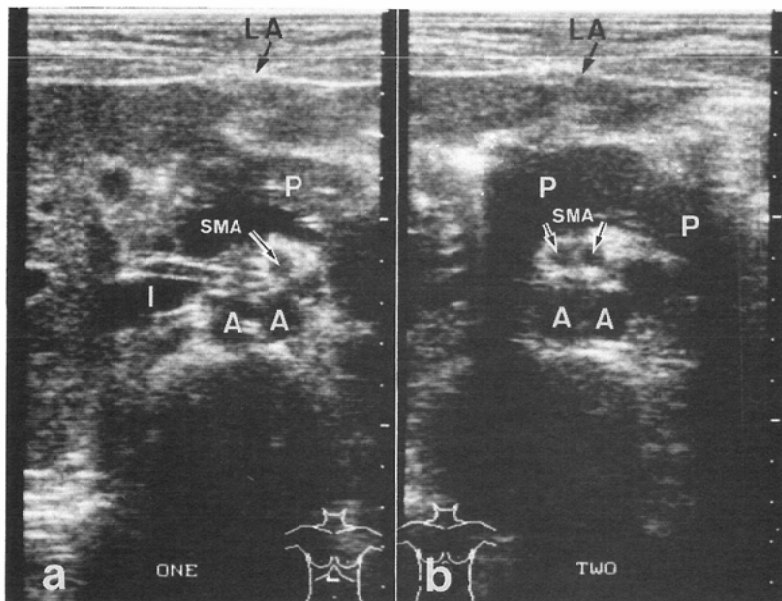


Fig. 2 Case 2. a, The superior mesenteric artery is visualized normally. b, The superior mesenteric artery is visualized as two round structures. Double images of the abdominal aorta are shown in Fig. 2a and 2b. A=aorta; I=inferior vena cava; SMA=superior mesenteric artery; P=pancreas LA=linea alba.

structures (Fig. 2b), when the superior mesenteric artery is located directly beneath the linea alba, Double images of the abdominal aorta are shown in Fig. 2a and 2b.

Case 3

The intrahepatic portal vein is visualized normally as in Fig. 3a, When the portal vein is located directly

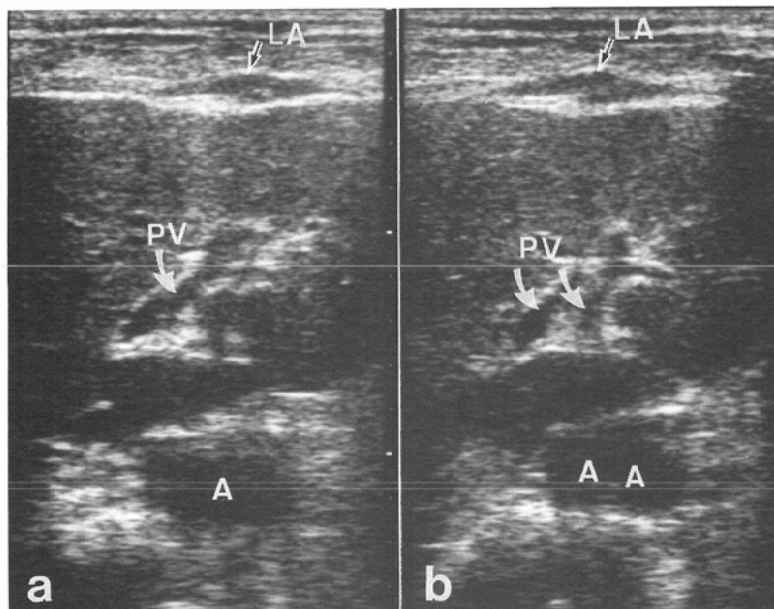


Fig. 3 Case 3. a, The intrahepatic portal vein is visualized normally. b, the umbilical portion of the portal vein is visualized as two channels. A=aorta; PV=portal vein; LA=linea alba.

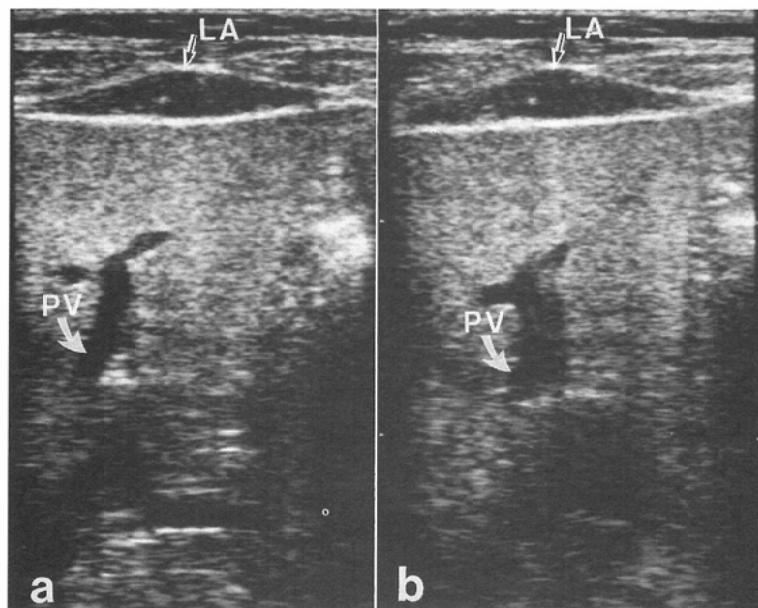


Fig. 4 Case 4. a, The umbilical portion of the intrahepatic portal vein is visualized normally, b, The portal vein appears dilated. PV=portal vein; LA=linea alba.

beneath the linea alba, the umbilical portion of the intrahepatic portal vein is visualized as two channels, rather than one (Fig. 3b).

Case 4

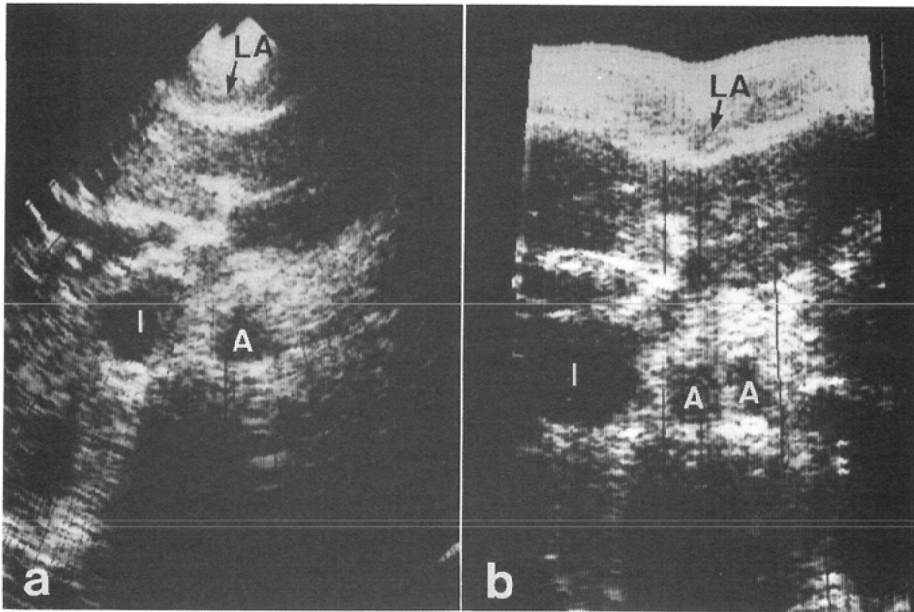


Fig. 5 Case 5. a, A sector scan made using a contact compound scanner. The abdominal aorta is normally visualized. b, A linear scan made using a contact compound scanner. The abdominal aorta is visualized as two round structures. A=aorta; I=inferior vena cava; LA=linea alba.

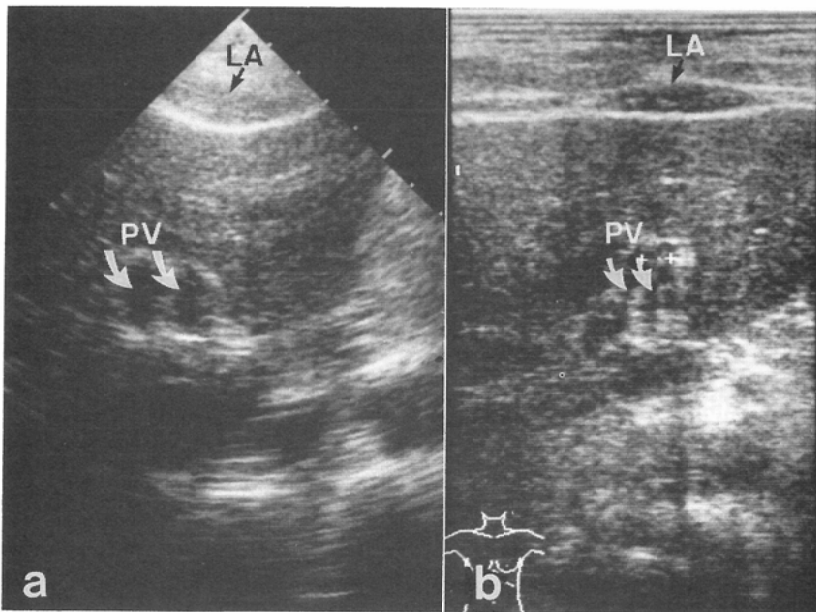


Fig. 6 Case 6. a, A sonogram made using a phased array. b, A sonogram made using a linear array. The umbilical portion of the intrahepatic portal vein is visualized as two channels in Fig. 6a and 6b. PV=portal vein; LA=linea alba.

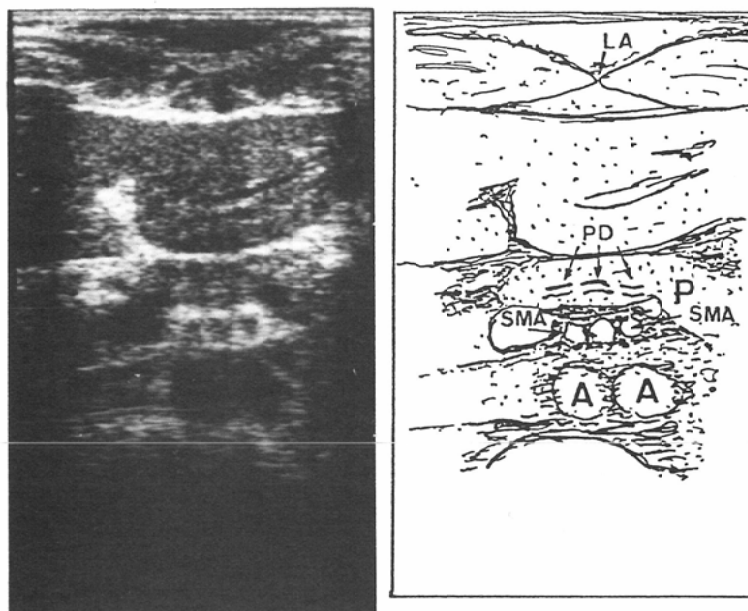


Fig. 7 Case 7. The superior mesenteric artery is visualized in three cross sections, the main pancreatic duct, in three portions. A= aorta; SMA=superior mesenteric artery; P=pancreas; PD=pancreatic duct; LA=linea alba.

The umbilical portion of the intrahepatic portal vein appears normal in Fig. 4a, but the portal vein appears dilated in Fig. 4b. In this case, the "ghost" image of the portal vein is adjacent to its real image.

Case 5

Fig 5a is a sector scan made using a contact compound scanner. The abdominal aorta is normally visualized. Fig. 5b is a linear scan made using a contact compound scanner. The abdominal aorta is visualized as two round structures.

Case 6

Fig. 6a is a sonogram made using a phased array. Fig. 6b is a sonogram scanned by a linear array. Both of these show the umbilical portion of the intrahepatic portal vein as two channels.

Case 7

The superior mesenteric artery is shown in three cross sections in Fig. 7. The central one is regarded the real image; the other two are "ghosts".

Experimental Study Using a Tissue Phantom

Lens effect artifacts were examined using a tissue-equivalent phantom.

1. Method and Materials

A phantom was constructed to simulate the upper portion of a human abdomen in cross-section, and was used to evaluate the effects of the lens phenomenon on ultrasonic beams. This phantom contained simulated rectus abdominis muscles, liver, and peritoneal fat, and is shown in Fig. 8.

"Ecobloc[®]", an ultrasonic phantom manufactured by the Acoustic Standard Corporation was used to simulate the liver. This material allows a sound velocity of 1,540 m/sec and an attenuation coefficient of 0.85 dB/cm MHz—the same specifications as normal human liver.

Olive oil was used to simulate fat because the sound velocity it permits is 1,445 m/sec, closely approximating the 1,450 m/sec of normal fat.

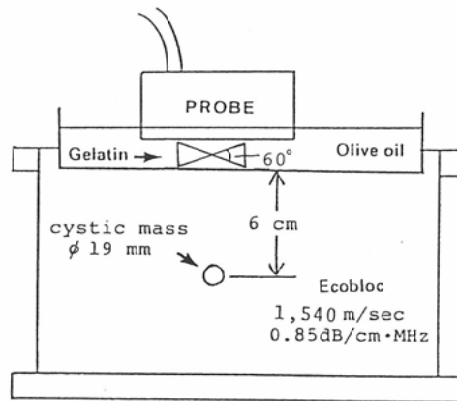


Fig. 8 Case 8. Tissue-equivalent phantom simulating the upper portion of a human abdomen in cross section.

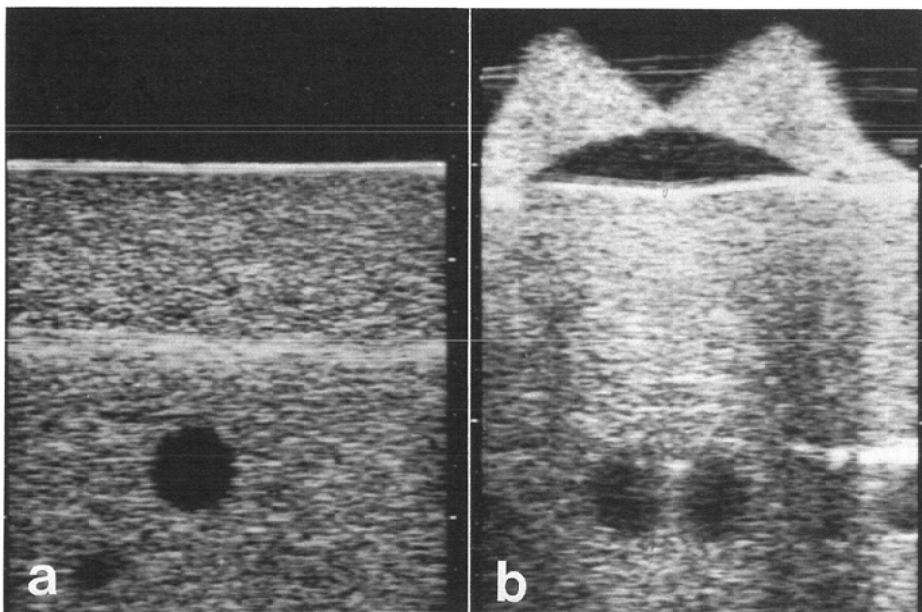


Fig. 9 Sonogram of the phantom scanned using a linear array. a, Without gelatin-gel, the echo-free circular inclusion is visualized as a round structures. b, With gelatin-gel, the echo-free circular inclusion is visualized as two round structures.

To simulate muscle, a gelatin-gel was mixed with n-propanol and graphite. The n-propanol regulated the sound velocity in the gel; the graphite controlled its echogenicity.

The gelatin phantom material was made according to the method of Ide²⁾, et al, whereby 20 gm gelatin powder were mixed with 170 ml water and 30 ml n-propanol. To this, 25 gm graphite were added, so that the gel's echogenicity approximated that of the "ecobloc[®]".

The gelatin gel was formed to simulate an isosceles triangle whose apical angle was 60 degrees.

2. Results

Fig. 9a shows a sonogram of the phantom without gelatin-gel scanned by a linear array. Note that the

image of the echo-free circular inclusion in the "ecobloc[®]" is free of the "lens effect" artifact.

Fig. 9b shows a sonogram of the phantom containing gelatin-gel. The echo-free circular inclusion is clearly visualized as a double image.

Fig. 10 shows a sonogram made using a phased array. Fig. 10a, made without gelatin-gel, shows an echo-free circular inclusion, normally visualized. Fig. 10b, made with gelatin-gel, shows an echo-free circular

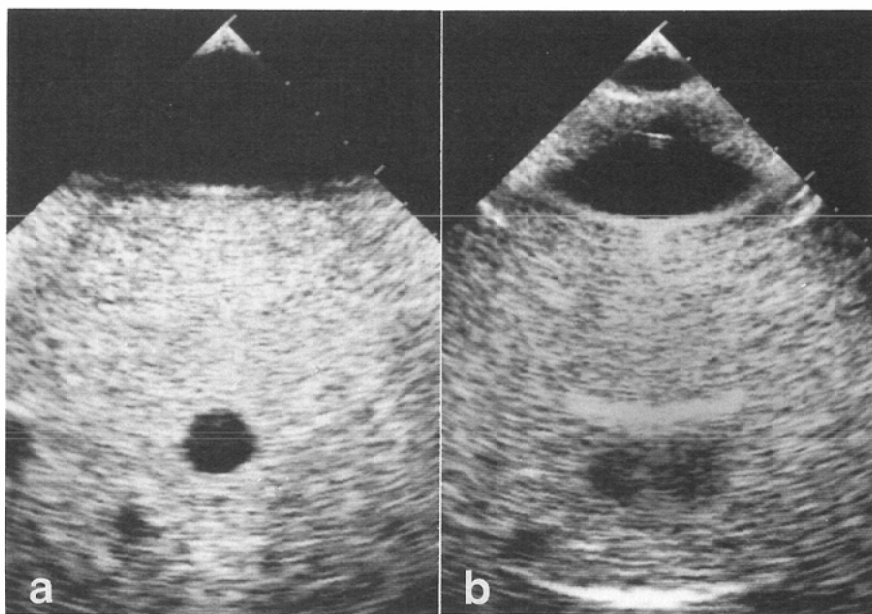


Fig. 10 Sonogram of the phantom scanned using a phased array. a, Without gelatin-gel, the echo-free circular inclusion is visualized as a round structure. b, With gelatin-gel, the echo-free circular inclusion is visualized as two round structures.

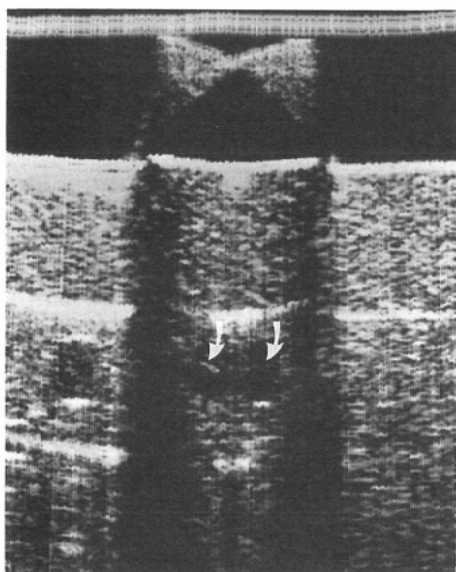


Fig. 11 Sonogram of the phantom with gelatin-gel made using a contact compound scanner. The echo-free circular inclusion is visualized as a double image.

inclusion which is visualized as a double image.

Fig. 11 shows a sonogram made using a contact compound scanner. With gelatin-gel, the echo-free circular inclusion is visualized as a double image.

Physics Involved in the Lens Effect

An ultrasonic beam obliquely incident on an interface between two different tissues is refracted in accord with Snell's law, as illustrated in Fig. 12. The angles and velocities are represented by the following expression;

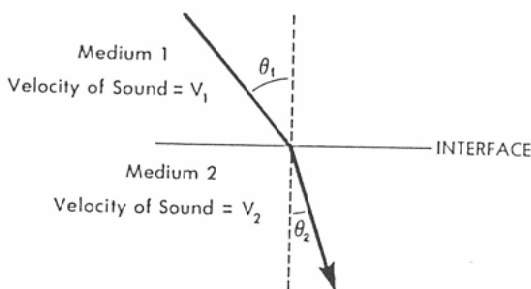
$$\frac{\sin \theta_2}{\sin \theta_1} = \frac{V_2}{V_1}$$

When an ultrasonic beam passes from a relatively low to a relatively high velocity medium, V_1 is less than V_2 . Therefore θ_1 is less than θ_2 , and the beam is refracted away from the perpendicular. When the ultrasonic beam passes from a high to a low velocity medium, V_1 is greater than V_2 , θ_1 is greater than θ_2 , and the beam is refracted toward the perpendicular.

Fig. 13 is a transverse ultrasonogram of the upper portion of a patient's anterior abdominal wall. The adjacent right and left rectus abdominis muscles are separated by the linea alba. In cross-section they resemble two convex optical lenses. Subcutaneous fat lines are anterior to the rectus abdominis muscles, and peritoneal fat is located between these muscles and the liver.

The velocity³⁾ of sound in fat is approximately 1,450 m/sec, in muscle, 1,585 m/sec, and liver, 1,550 m/sec. The sound velocity in fat is obviously less than that in muscle and liver. These differences in sound velocities result in refraction of the ultrasonic beam at interfaces. During a transverse scan of the upper portion of the abdomen in midline, an acoustic lens is formed by the rectus abdominis muscles, fat, and the liver, which refract the ultrasonic beam.

Refraction of the ultrasonic beam around the rectus abdominis muscles is illustrated in Fig. 14. The formula for calculating the final refraction angle, θ_6 , is shown below. In cross section each rectus abdominis muscle has a curved contour which juts exteriorly; however, in this case, a straight line has been substituted for this surface to facilitate calculations, and a triangular column has been substituted for each rectus abdominis muscle. The angle formed by the anterior surface of the rectus abdominis muscle and a line parallel with the skin is represented by θ_A . The angle formed by the posterior surface of the rectus abdominis muscle and a line parallel with the skin is represented by θ_B . The angle formed by the posterior surface of the peritoneal fat and a line parallel with the skin is represented by θ_C . The following relations obtain;



$$\text{SNELL'S LAW} \quad \frac{\sin \theta_2}{\sin \theta_1} = \frac{V_2}{V_1}$$

Fig. 12 Snell's law.

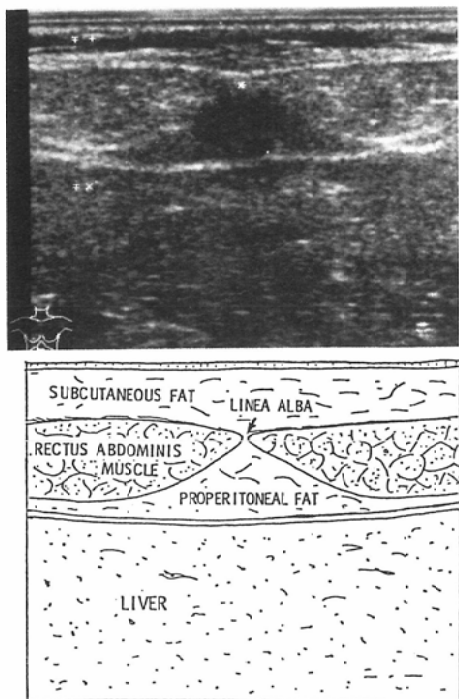


Fig. 13 Transverse sonogram of the upper portion of the abdomen.

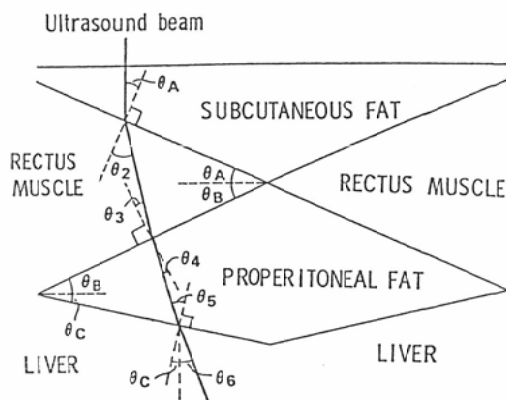


Fig. 14 Refraction of the ultrasonic beam around the rectus abdominis muscle.

$$\frac{\sin \theta_2}{\sin \theta_A} = \frac{V_m}{v_f} \quad V_m = \text{sound velocity of the muscle}$$

$$\frac{\sin \theta_4}{\sin \theta_3} = \frac{V_f}{V_m} \quad V_f = \text{sound velocity of the fat}$$

$$\frac{\sin (\theta_C + \theta_6)}{\sin \theta_5} = \frac{V_l}{V_f} \quad V_l = \text{sound velocity of the liver}$$

$$\theta_2 + \theta_3 = \theta_A + \theta_B$$

$$\theta_4 + \theta_5 = \theta_B + \theta_C$$

The final refraction angle, θ_6 , is determined as follows:

$$\theta_6 = \sin^{-1} \left\{ \frac{V_l}{V_f} \sin [\theta_B + \theta_C - \sin^{-1} \left(\frac{V_f}{V_m} \sin \{ \theta_A + \theta_B - \sin^{-1} \left(\frac{V_m}{v_f} \sin \theta_A \} \right) \right)] \right\} - \theta_C$$

When the ultrasonic beam is refracted at the rectus abdominis muscle near the linea alba and is propagated obliquely in the body, some of the beam is reflected and returns to the transducer by the same route, as shown in Fig. 15.

After this reflected ultrasonic beam is electronically processed, it is displayed immediately posterior to the point where the ultrasonic beam passed through the skin. As a result, the reflector in the body is displayed away from its true position. The distance of its displacement is equal to half of the distance "d" in Fig. 15.

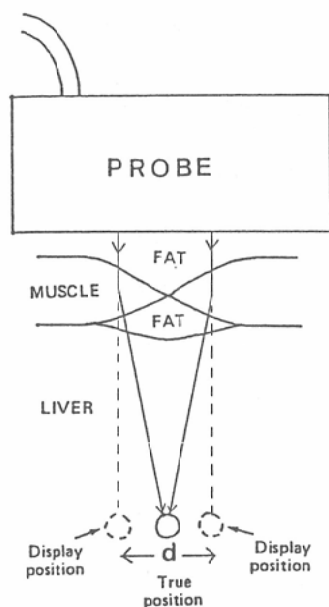


Fig. 15 Principle of the double image. When the ultrasonic beam is refracted at the rectus abdominis muscle and is propagated obliquely along the solid line, the image of the target is displayed as if the ultrasonic beam is propagated along the dotted line.

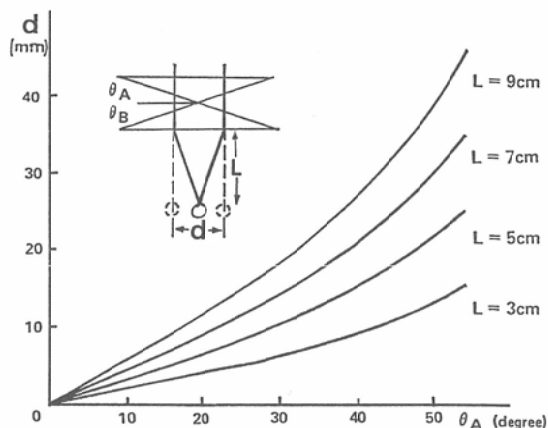


Fig. 16 Theoretical distance between the two "ghost" images. The horizontal axis represents the angle of the rectus abdominis muscle; the vertical axis indicates the distance between the two "ghost" images (d). The correlation between the angle of the rectus abdominis muscle and the distance between the "ghost" images is expressed according to depth " L ". Here, it has been assumed that θ_A equals θ_B and that θ_C equals zero.

The ultrasonic beam, which is refracted by the right rectus abdominis muscle, images the reflector toward the right, and the ultrasonic beam which is refracted by the left rectus abdominis muscle images the reflector toward the left. As a result, two "ghost" images are visualized instead of the real image.

If an ultrasonic beam is transmitted through the linea alba, three images—one real and two apparent ("ghosts")—are visualized. This occurs only when the reflector is relatively small and the linea alba is sufficiently wide.

In Fig. 16, the distance between the two "ghost" image is indicated theoretically.

The horizontal axis represents the angle of the rectus abdominis muscle; the vertical axis, the distance between the two "ghosts". The correlation between the angle of the rectus abdominis muscle and the distance between the ghosts is expressed according to depth. Here, it was assumed that θ_A equals θ_B , and that θ_C is zero.

In the clinical situation, the distance between the two "ghosts" on film was compared with the theoretical distance obtained by calculation. The subjects were 12 patients for whom clear images of their rectus abdominis muscles were obtained. The angles of their rectus abdominis muscle, θ_A , θ_B , and peritoneal fat, θ_C , were measured on the films in the right and left muscles as shown in Fig. 14. The final refraction angle, θ_6 , was calculated according to the expression, and the distance between the "ghosts" was obtained by multiplying $\tan \theta_6$ by the depth of the target and by adding the two values. The results are shown in Table 1. The distances calculated correlate well with the distances measured on the films.

Table 1 Distance between "ghost" images by calculation and as measured on film.

age	sex	θ_A	θ_B	θ_C	θ_0	depth of target	calculated distance	measured distance
24	F	Rt)	15°	20°	0°	50mm	5.5mm	6mm
		Lt)	17.5	15	0			
49	M		22.5	25	5	59	9.3	7
			20	20	5			
48	F		17.5	10	12.5	50	5.2	8
			10	17.5	0			
39	M		17.5	10	17.5	77	10.6	14
			15	25	5			
49	M		7.5	10	7.5	50	4.5	8
			10	20	5			
33	M		15	20	5	78	12.0	10
			15	35	5			
44	F		12.5	17.5	2.5	50	6.5	8
			22.5	27.5	-5			
39	M		10	25	7.5	110	21.0	19
			15	27.5	5			
53	M		5	12.5	2.5	30	4.8	6
			5	10	2.5			
19	F		20	25	7.5	50	8.7	12
			17.5	25	15			
36	M		12.5	15	12.5	62	8.2	12
			15	20	12.5			
16	F		22.5	25	15	50	8.3	9
			10	30	0			

Vm=1,585m/s Vf=1,450m/s V1=1,550m/s

Discussion

Several kinds of artifacts are encountered in ultrasonographic images⁴⁾⁵⁾, including the well known reverberation echo, side lobe artifacts, lateral shadow⁶⁾⁷⁾ and the mirror image artifact. The reverberation echo is a "ghost" image resulting when the ultrasonic beam is reflected between multiple strong reflectors and the transducer surface. Side lobe artifacts are due to the presence of multiple transducer side lobes, and strong reflectors which are located off the beam axis but which are displayed on the main beam axis. A lateral shadow⁶⁾⁷⁾ results from a refracted ultrasonic beam when it strikes a curved lateral surface of a round structure. Mirror image artifacts occur in the vicinities of highly reflective acoustic interfaces, such as the diaphragm and the lung. In the latter artifact, the ultrasound is reflected out of the beam axis to an off-axis reflector.

This is a report of the "lens effect" artifact which is produced during transverse scans, in which the structures in midline are visualized as double images. During 62 clinical abdominal ultrasonographic examinations in which this artifact was recognized, it was produced when the target was located directly beneath the linea alba, while controlling the patient's respirations and the probe's angulation. The artifact disappeared whenever the direction of the ultrasonic beam was changed.

Experimental studies using a tissue-equivalent phantom simulating the upper portion of a human abdomen resulted in visualization of an echo-free circular inclusion in the simulated liver as a double image, but only when it was located directly beneath the junction of the simulated rectus abdominis muscles.

By applying Snell's law to sound velocity data for human tissues, the refraction angle of the ultrasonic beam was calculated, and the paths of the ultrasonic beam in the body were plotted assuming that the examination was performed using a linear array. It was clear that the ultrasonic beam was refracted toward midline near the linea alba. It was also confirmed that small structures immediately beneath the surface in midline are displayed as two images side-by-side in a transverse ultrasonogram. This proved that this artifact is produced by refraction of the ultrasonic beam as it passes through the rectus abdominis muscle.

We have termed this artifact the "lens effect" because the rectus abdominis act as an acoustic lens in producing it.

Theoretically, the lens effect phenomenon can be produced using contact compound scanners when linear scans are made. This was confirmed by experimental study using the tissue-equivalent phantom, and was proved during clinical studies. When a transverse scan is made in midline using a contact compound scanner, a sector scan is generally used, and a perfect linear scan is seldom obtained. For this reason, the lens effect phenomenon is not usually encountered during examinations using contact compound scanners.

Theoretically, when a phased array is used, the lens effect phenomenon occurs in a limited number of cases. The ultrasound beam diverges in the shape of an unfolded fan, and the angle incident on the rectus abdominis muscle is much less than that described by a beam of a linear array. For this reason, when a phased array is used, the ultrasonic beam passing through the rectus abdominis muscle is not always refracted toward midline. If the rectus abdominis muscles are sufficiently well developed, the ultrasound beam is refracted toward midline, and the target directly beneath the linea alba is visualized as a double image.

In 1984, Buttery and Davison⁸⁾ reported "the ghost artifact" produced by the rectus abdominis muscles in transverse sonograms of pelvic organs, pointing out that the rectus abdominis muscle acts as a lens and refracts the ultrasonic beam. They concluded that the refraction is caused by the configuration of two "lenses" of low velocity separated by tissues of high velocity—the linea alba and the rectus sheath. However, the present study showed that the configurations of two lenses of high velocity separated by tissues of low velocity, the subcutaneous fat and the peritoneal fat, are all responsible for the refraction of the ultrasonic beam. Furthermore, the present study confirmed that the direction of the refraction of the ultrasonic beam passing through the rectus abdominis muscles is opposite to that which Buttery and Davidson reported. In 1984, Müller et al⁹⁾ reported "the double image artifact", the same phenomenon as is usually observed in the uterus, and they arrived at a conclusion similar to ours concerning its mechanism.

In their study only a realtime mechanical sector scanner was used; whereas, linear array, phased array and contact compound scanners were used in the present study.

Judging from the physics involved in the lens effect, the double image phenomenon occurs within a very narrow field beneath the linea alba. This was confirmed in the present study, both by experiment using a tissue-equivalent phantom and by clinical observations.

The lens effect artifact is recognized not only at the medial edge of each rectus abdominis muscle but in other body sites where muscle thicknesses vary; for example, at the lateral margins of the rectus abdominis muscle during transverse scans, and in the transverse connective tissue between the segments of the rectus abdominis muscle, during longitudinal scans.

The main pancreatic duct is often clearly visualized as a 1 to 2 cm long structure in midline. With the lens effect, the main pancreatic duct may appear longer than it actually is. Case seven strongly suggests this possibility.

This report involves mainly the rectus abdominis muscles as a cause of the lens effect. Rib cartilages can also act as lenses when a scan traverses them, distorting the gallbladder wall, the renal contours, and producing double images of the intrahepatic portal vein. We must be alert for these conditions in order to avoid misinterpretations and erroneous diagnoses.

The lens effect is clearly recognized when the rectus abdominis muscles are relatively well developed and there is sufficient peritoneal fat; When the patient is not obese, and has relatively little intestinal fat. It is seen when structures such as the intrahepatic portal vein, superior mesenteric artery and the aorta have discrete contours and are clearly visualized; and when the clearly defined structures are located directly beneath the linea alba.

The lens effect phenomenon is clinically significant because of the problem arising when structures are visualized as double images. For example, when a tributary of the intrahepatic portal vein appears as a double image, it can be misinterpreted as a parallel channel¹⁰⁾ or a hypoechoic mass. When the superior mesenteric artery appears as a double images, one of the images can be mistaken for a superior mesenteric vein or an anomalous vessel. when the aorta is visualized as a double image, it can be misdiagnosed as a dissecting aneurysm.

Acknowledgement

Gratitude is expressed to Walter J. Russell, M.D., Chief of the Department of Radiology, Radiation Effect Foundation, Hiroshima, for reviewing and editing the manuscript.

Reference

- 1) Goldstein, A. and Madarazo, B.L.: Slice-thickness artifacts in gray-scale ultrasound. *J. Clin Ultrasound* 9: 365—375, 1981
- 2) Ide, M., Ohdaira, E. and Masuzawa, N.: Study on phantom for B-mode ultrasonic equipment. *The Japan Society of Ultrasound in Medicine Proceedings* 36: 435—436, 1980
- 3) Buddemeyer, E.U.: The physics of diagnostic ultrasound. *Radiologic Clinics of North America* 13: 391—415, 1975
- 4) Laing, F.C.: Commonly encountered artifacts in clinical ultrasound. *Seminars in Ultrasound* 4: 27—43, 1983
- 5) Robinson, D.E.: Artifacts (In) Vlieger, M., Holmes, J.H., Kartowil, A., Hazner, E., ed: *Handbook of clinical ultrasound*. 55—58, 1978, John Wiley & Sons, New York
- 6) Sommer, F.G., Filly, R.A. and Minton, M.J.: Acoustic shadowing due to refraction and reflection effects. *Am J Roentgenol* 132: 973—977, 1979
- 7) Robinson, D.E., Wilson, L.S. and Kossoff, G.: Shadowing and enhancement in ultrasonic echogram by reflection and refraction. *J Clin Ultrasound* 9: 181—188, 1981
- 8) Buttery, B. and Davison, G.: The ghost artifact. *J Ultrasound Med* 3: 49—52, 1984
- 9) Müller, N., Cooperberg, P.L., Rowley, V.A., Mayo, J., Ho, B. and Li D.K.B.: Ultrasonic refraction by the rectus abdominis muscle: the double image artifact. *J Ultrasound Med* 3: 515—519, 1984
- 10) Conrad, M.R., Landay, M.J. and Janes, J.O.: Sonographic "parallel channel" sign of biliary tree enlargement in mild to moderate obstructive jaundice. *Am J Roentgenol* 130: 279—286, 1978